Vol. 18, No. 2 (2019) 513-529
Revista Mexicana de Ingeniería Química

PYRENE BICHROMOPHORES SUPPORTED ON POLYMER BEADS: A NEW LIBRARY OF FLUORESCENT MATERIALS FOR SENSING HEAVY METALS IN WATER

BICROMÓFOROS DE PIRENO SOPORTADOS EN PERLAS DE POLÍMEROS: UNA NUEVA BIBLIOTECA DE MATERIALES FLUORESCENTES PARA LA DETECCIÓN DE METALES PESADOS EN AGUA

J.E. Ávila-Manzanares, H. Santacruz, L. Machi*

Departamento de Investigación en Polímeros y Materiales, Universidad de Sonora, Hermosillo, Sonora, México.

Received: August 13, 2018; Accepted: October 19, 2018

Abstract

A new combinatorial library of fluorescent materials was prepared by covalent anchoring of 1-pyrene and 1-methylpyrene bichromophores to Merrifield and Wang resins functionalized with alkyl diamine spacers and its sensing properties toward Pb^{2+}, Cd^{2+} and Hg^{2+} were evaluated in water. It was found that the Wang resin modified with ethane-1,2-diamine as spacer and functionalized with the 1-pyrene bichromophore senses selectively Pb^{2+} with an enhancement of fluorescence intensity. The detection limit and the percentage of sorption were determined as 29.6 μM and 80.3%, respectively.

Keywords: Pyrene bichromophores, fluorescent probe, chemical sensors, heavy metals.

Resumen

Se preparó una nueva biblioteca combinatoria de materiales fluorescentes mediante el anclaje covalente de dos bicromóforos de pireno (derivados de 1-pireno y 1-metilpireno, respectivamente) a resinas Merrifield y Wang funcionalizadas con espaciadores de tipo alquildiamina y se evaluaron sus propiedades de detección de los metales Pb^{2+}, Cd^{2+} y Hg^{2+} en agua. Se encontró que la resina Wang modificada con el espaciador etano-1,2-diamina y funcionalizada con el bicromóforo de 1-pireno detecta selectivamente a Pb^{2+} con un aumento en la intensidad de fluorescencia. Se determinaron el límite de detección y el porcentaje de sorción como 29.6 μM y 80.3%, respectivamente.

Palabras clave: Bicromóforos de pireno, sonda fluorescente, sensores químicos, metales pesados.

1 Introduction

Nowadays, the design and preparation of fluorescent sensors is a research topic of great interest because of the high demand that these devices have in fields such as analytical chemistry, clinical biochemistry and medical research. One strategy to development of this kind of devices consists in the covalently attachment of fluorescent chemosensors (molecules whose fluorescence emission changes in response to a binding event) to the surface of solid supports (Akhila Maheswari and Subramanian, 2003; Kara, 2005; Narin *et al*., 2003; Prabhakaran and Subramanian, 2003; Xie *et al*., 2014).

The anchoring would result in improved analytical properties, such as continuous readouts, increased sensitivity, lower reagent consumption, and the possibility of using the sensor in solvents in which the free molecule may display low solubility. Resin bound fluorescent chemosensors for several analytes have been made by combinatorial methods (Aguilar-Martínez *et al*., 2013; Brown *et al*., 2008; Castillo and Rivero, 2004; Joshi *et al*., 2007; Joshi *et al*., 2014; Nath and Maitra, 2006; Rivero *et al*., 2004; Santacruz Ortega *et al*., 2009). A variety of fluorescent motifs have been employed on the design of those materials, including dansyl group (Joshi *et al*., 2014), anthracene (Brown *et al*., 2008; Castillo and Rivero, 2004), aminenaphthalene sulfonic acid (Santacruz Ortega *et al*., 2009) and pyrene (Nath and Maitra, 2006).

* *Corresponding author. E-mail*: lmachi@polimeros.uson.mx
Tel. +521-662-2592161
https://doi.org/10.24275/uam/izt/dcbi/revmexingquim/2019v18n2/Avila
issn-e: 2395-8472

Fluorescent chemosensors based on pyrene have attracted considerable attention due to their well-known photophysical properties (Chen *et al*., 2010; Hou *et al*., 2011; Hung *et al*., 2009; Lodeiro *et al*., 2006; Machi *et al*., 2009; Manandhar and Wallace, 2012; Pérez-González *et al*., 2011; Thirupathi and Lee, 2013; Yang *et al*., 2011; Zhou *et al*., 2010). Particularly, the introduction of two pyrene moieties at the ends of interlinking chains containing electron donating atoms has given a number of sensing systems capable of switch the monomer/excimer emission upon coordination with specific guest ions (Chen *et al*., 2010; Lodeiro *et al*., 2006; Machi *et al*., 2009; Pérez-González *et al*., 2011; Zhou *et al*., 2010). Previously, we reported two water-soluble 1-pyrene and 1-methylpyrene bichromophores, (**ttha1py**)$\mathbf{H_4}$ and (**ttha1mpy**)$\mathbf{H_4}$ (**1py** and **1mpy**, Scheme I), in which two pyrenyl groups are linked by an triethylenetetraminehexaacetic acid unit (TTHA) (Pérez-González *et al*., 2011). The derivatives exhibit emission bands of monomeric pyrene between 393 and 414 nm and an intense structureless excimer band at 487 nm. The fluorescence of the molecules in aqueous solution is very sensitive to changes in pH and to the presence of transition metal ions (Avila M., 2012; Pérez-González *et al*., 2011). In the present work, we report the immobilization of derivatives **1py**(**x**) and **1mpy**(**y**) in Merrifield (m) and Wang (w) resins with alkyl diamines spacers of different length: ethane-1,2-diamine (a), butane-1,4-diamine (b), hexane-1,6-diamine (c) and octane-1,8-diamine (d), to obtain a combinatorial library of 16 fluorescent materials **1**(**m**, **w**)(**a** – **d**)(**x**, **y**) (Scheme I).

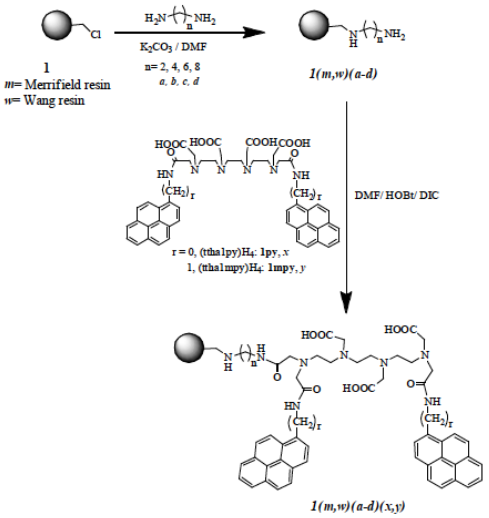

Scheme I

The fluorescence and the sensing properties in water of these materials toward the toxic metal ions Pb^{2+}, Cd^{2+} and Hg^{2+} were studied. Results demonstrated that Wang resins modified with 1,2-, 1,4- and 1,6-diaminoalkanes as spacers and functionalized with **1py**, **1w**(**a** – **c**)**x**, respond in a selective form to Pb^{2+} with an increase in emission intensity. More important, the resin **1wax** maintains the fluorescence enhancement by coordination to Pb^{2+} even in presence of Hg^{2+} and Cd^{2+}.

The detection limit and the percentage of sorption of **1wax** toward Pb^{2+} were determined as 29.6 μM and 80.3%, respectively. The sorption capability of **1wax** remains constant for at least 10 cycles, which makes it a potential sensor of Pb^{2+} in aqueous media.

2 Materials and methods

2.1 *Materials*

Merrifield-Cl with 1.5 mmol/g loading, 2% cross-linked with divinylbenzene, Wang-Cl with 1.5 mmol/g loading, 1% cross-linked with divinylbenzene, 1,4-diaminobutane (99%), 1,6-diaminohexane dihydrochloride (99%), 1,8-diaminooctane (98%), 1-hydroxybenzotriazole hydrate (HOBt, 97%) and *N,N'*-dimethylformamide (DMF) were purchased from Aldrich. 1,2- diaminoethane (99%), *N,N'*-diisopropylcarbodiimide (DIC, 99%), 3-(N-morpholino)propanesulfonic acid (MOPS, 99%), cadmium(II) chloride (99%) and lead(II) chloride (99%) were purchased from Sigma. Mercury(II) chloride (99%) was purchased from Mallinckrodt. All chemicals and solvents were of analytical reagent grade and were used without further purification.

2.2 *Instrumentation*

Infrared (IR) spectra were recorded on a Perkin-Elmer FT-IR GX and on a Perkin-Elmer Spectrum Two module UATR spectrometers. The samples were analyzed in KBr pellets. Raman spectra were recorded on a Horiba Scientific LabRam HR Evolution Raman microscope using a laser of 632.8 nm. Fluorescence spectra were recorded on a Perkin-Elmer LS50B luminescence spectrometer. Measures of fluorescence intensity were obtained directly from the resin beads packing into a Hellma model 176.753-QS flow-through fluorescence microcell (8 μL).

Table 1. Quantities of products **1**(**m**, **w**)(**a** – **d**) obtained (in grams), yield of reactions (in %) and frequencies (in cm^{-1}) of the characteristic stretching peak of secondary N–H amine in the IR spectra of the materials.

Resin	Product quantity	Yield	Frecuency N–H
1ma	0.246	98	3307
1mb	0.234	93	3319
1mc	0.221	88	3360
1md	0.213	85	3328
1wa	0.583	97	3356
1wb	0.556	92	3372
1wc	0.571	95	3344
1wd	0.535	89	3356

For determination of final concentrations of Pb^{2+} (C_f) in the sorption studies, a Perkin Elmer Analyst 400 flame atomic absorption spectrometer was employed. Atomic absorption measurements were carried out in air/acetylene flame. All measurements were carried out at 25 °C.

2.3 *General method for the synthesis of alkyl diamine-modified resins*

Merrifield-Cl resin (0.250 g, 1.5 mmol/g, 0.375 mmol, 1 eq) was swollen in DMF (15 mL) for 0.5 h at 25 °C. K_2CO_3 (0.208 g, 4 eq) and the appropriate alkyl diamine (4 eq) were added and the reaction was placed on a shaker for 72 h at 25 °C. The resin was filtered and washed with DMF (4x15 mL), water (3x15 mL) and acetone (3x15 mL) and dried under vacuum for 10 h. This process provided free flowing resins that gave a positive Kaiser test. The products were characterized by Raman and infrared (IR) spectroscopies. The total conversion of chloro residues in Merrifield resin into alkyl diamine groups was 99% for **1m**(**a**, **b**), 97% for **1mc** and 98% for **1md**, as reveled the Raman spectroscopy studies. Derivatization of Wang resin was done following the same methodology as with Merrifield-Cl resin starting from 0.600 g of Wang-Cl resin (1.5 mmol/g, 0.900 mmol, 1 eq). The products, obtained as free flowing resins that gave a positive Kaiser test, were characterized by Raman and IR spectroscopies.

The total conversion of chloro residues in Wang resin into alkyl diamine groups was 97% for **1w**(**a**, **b**, **d**) and 96% for **1mc**, as reveled the Raman spectroscopy studies. The quantities of products **1**(**m**, **w**)(**a** – **d**) obtained (in grams), the yields of reactions (in %) and the frequencies (in cm^{-1}) of the characteristic stretching peak of secondary N–H amine in the IR spectra of the materials are shown in Table 1.

2.4 *General method for anchoring the ligands on the alkyl diamine-modified resins*

Alkyl diamine-modified Merrifield resin (0.100 g, 0.15 mmol, 1 eq) was swollen in DMF (15 mL) for 0.5 h at 25 °C. **1py** or **1mpy** (1.1 eq), HOBt (0.090 g, 4 eq) and DIC (0.103 mL, 4 eq) were added and the reaction was placed on a shaker for one week at 25 °C. The resin was filtered and washed with DMF (4x15 mL), water (3x15 mL) and acetone (3x15 mL) and dried under vacuum for 10 h. This provided free flowing beads that were characterized by IR and fluorescence spectroscopies. Immobilization of ligands **1py** and **1mpy** on alkyl diamine-modified Wang resins was done following the same methodology as with Merrifield resins starting from 0.100 g of derivatized Wang resins (0.15 mmol, 1 eq). The products were characterized by IR and fluorescence.

The quantities of final products **1**(**m**, **w**)(**a** – **d**)(**x**, **y**) obtained (in grams), the yields of reactions (in %) and the frequencies (in cm^{-1}) of the characteristic stretching peak of secondary N–H amine and C=O of carbonyl in the IR spectra of the materials are shown in Table 2.

2.5 *General methods for the evaluation of the sensing properties*

To 0.030 g (0.045 mmol, 1 eq) of sensor material, the appropriate volume of 0.01 M solution of the metal to be coordinated was added to obtain a ratio of 2.1 equivalents with respect to the loading of the resin. The metal solutions were prepared in buffer MOPS at pH 7.9 for $HgCl_2$ and $CdCl_2$ and pH 5 for $PbCl_2$. After shaking for 48 h at 25°C, the resin was washed with water (3x15 mL), filtered and dried under vacuum for 24 h. Subsequently, the resin was packed into a flow-through fluorescence microcell and fluorescence spectra recorded. The experiments were performed in triplicate. Methodology for competition in binary and ternary mixtures: For the binary tests, the fluorescent material [**1w**(**a** – **c**)**x**], was first put in contact with the competitor metal ion (Cd^{2+} or Hg^{2+}) and subsequently treated with Pb^{2+}.

Table 2. Quantities of final products **1**(**m**, **w**)(**a** − **d**)(**x**, **y**) obtained (in grams), yield of reactions (in %) and frequencies (in cm^{-1}) of the characteristic stretching peaks of N−H amide and C=O of carbonyl in the IR spectra of the materials.

Resin	Product quantity	Yield	Frequency	
			N−H	C=O
1max	0.0792	79	3446	1676, 1602
1mbx	0.0978	97	3418	1698, 1602
1mcx	0.0726	72	3418	1678, 1602
1mdx	0.0803	80	3418	1678, 1602
1may	0.0822	82	3414	1680, 1602
1mby	0.0964	96	3334	1646, 1602
1mcy	0.09	90	3446	1678, 1602
1mdy	0.083	83	3350	1674, 1602
1wax	0.0933	93	3286	1676, 1646
1wbx	0.0962	96	3316	1668, 1648
1wcx	0.0883	88	3364	1698, 1680
1wdx	0.0964	96	3364	1666, 1644
1way	0.091	91	3334	1664, 1650
1wby	0.0924	94	3286	1706, 1650
1wcy	0.0983	98	3416	1710, 1678
1wdy	0.0942	94	3334	1664, 1650

In addition, each material was treated independently with Pb^{2+} to be used it as reference. The ternary competition test was carried out for the resin **1wax**. The material was first put in contact with the competing metals sequentially (first with Hg^{2+} and then with Cd^{2+}) and finally treated with Pb^{2+}. In addition, **1wax** was treated independently with Pb^{2+}, to be used it as reference. At each stage of the tests, the fluorescent materials were treated according to methodology described above, using an excess of 9 eq. of metal, and the experiments were performed in duplicate. For determination of detection limit of **1wax** towards Pb^{2+}, five samples of the resin were treated with increasing concentrations of Pb^{2+} (0 μM, 750 μM, 1500 μM, 2200 μM, 3000 μM) following the methodology describe above. After washing and vacuum drying, the resins were packed into a flow-through fluorescence microcell and the spectra recorded. The experiments were performed in duplicate and the averages of fluorescence intensities were plotted against the concentration of Pb^{2+}. The *DL* was calculated with Ec. 1.

$$DL = 3\sigma/m \tag{1}$$

where σ is the standard deviation of blank measurements and m is the slope of the plot of intensity versus Pb^{2+} concentration.

2.6 *Sorption properties of* **1wax** *toward* Pb^{2+} *ion*

For determination of the percentage of sorption of Pb^{2+} (% Sorption) and for studies of reusability and stability of the resin **1wax**, the column technique was used. In a glass column (0.5 cm x 10 cm), 0.02 gr of the **1wax** ware placed and fixed with a small amount of cotton. A standard solution of $PbCl_2$ (20 mL, 9 ppm, pH 5, buffer MOPS,) was passed through the column using a peristaltic pump at a flow rate of 1.2 mL/min. After passing through the column, the metal solution was collected and the final concentration of Pb^{2+} was determined by atomic absorption spectroscopy. The experiments were performed in triplicate. The % Sorption was calculated from the following equation:

$$\%\ Sorption = [(C_i - C_f)/C_i] \cdot 100 \tag{2}$$

where C_i is the initial concentration of Pb^{2+} in the standard solution (in ppm) and C_f is the final concentration after the sorption.

The stability and regeneration capacity of **1wax** after repeated cycles of sorption-desorption of Pb^{2+} ions were determined following the column technique describe above. After each sorption cycle, the column was washed with 5 mL of 1% HNO_3 and 5 mL of deionized water for regeneration of the resin. This process was repeated 10 times on the same sample without a significant loss of sorption capacity being observed.

3 Results and discussion

3.1 Preparation of the materials

Merrifield and Wang resins functionalized with alkyl diamines ethane-1,2-diamine, butane-1,4-diamine, hexane-1,6-diamine and octane-1,8-diamine [**1**(**m**,**w**)(**a** – **d**), Scheme I], were prepared according to the method reported by Rivero (Rivero *et al*., 2004). The formation of alkyl diamine-modified resins was monitored by Raman and IR spectroscopy (see spectra in Appendix A). Additionally, the Kaiser test for primary amines was done for each material, giving positive results (Gaggini *et al*., 2004). The Raman spectra of the modified resins **1**(**m**,**w**)(**a** – **d**) do not show the stretching peak of C−Cl bond neither the wagging peak of the methylene $-CH_2-Cl$, which are present in the spectra of unmodified resins (Merrifield: C−Cl at 677 cm^{-1} and $-CH_2-Cl$ at 1263 cm^{-1}; Wang: 666 and 1264 cm^{-1}) (Figures A1 and A2) (Larkin, 2011; Yan *et al*., 1998).

On the other hand, the infrared spectra of modified resins showed the characteristic stretching peak of secondary N−H amine at about 3300 cm^{-1} and the absence of the C−Cl peak, which is present in the spectra of native resins (Merrifield C−Cl peak at 874 cm^{-1}; Wang: 668 cm^{-1}) (Figures A3 and A4). These results indicate that the bidentate amines were successfully attached into the native resins. The next step was to anchor the ligands **1py** or **1mpy** to the modified resins **1**(**m**,**w**)(**a** – **d**) through the formation of amide bonds between the primary amine group in the spacers and the carboxymethyl groups of the ligands. To resins **1**(**m**,**w**)(**a** – **d**) suspended in DMF, the ligands in their acidic forms and the coupling reagents DIC and HOBt were added. After one week of reaction, the materials **1**(**m**,**w**)(**a** – **d**)(**x**,**y**) were obtained as free flowing beads which were characterized by IR and fluorescence spectroscopy.

Table 3. Fluorescence spectra data of native Merrifield and Wang resins **1(m,w)**, resins modified with diamine spacers [**1**(**m**,**w**)(**a** – **d**)] and the final products [**1**(**m**,**w**)(**a** – **d**)(**x**,**y**)].

Resin	λ_{max} (nm)		$I_R^{a,b}$	Resin	λ_{max} (nm)		I_R^a
	Excitation	Emission			Excitation	Emission	
1m	340	405	1	**1w**	389	448	1
1ma	337	406	0.68 (0.18)	**1wa**	392	457	0.64
1mb	339	402	0.77 (0.85)	**1wb**	390	449	0.71
1mc	338	405	0.48 (0.92)	**1wc**	390	448	0.85
1md	337	402	0.60 (0.88)	**1wd**	388	448	0.75
1max	393	450[c]	0.31	**1wax**	398	483	1.28
1mbx	397	469[c]	0.09	**1wbx**	399	479	1.51
1mcx	383	414	0.33	**1wcx**	387	410	1.21
1mdx	389	425	0.23	**1wdx**	395	479	1.16
1may	391	482[c]	0.04	**1way**	383	491	0.82
1mby	391	500[c]	0.03	**1wby**	385	491	1.33
1mcy	387	418	0.43	**1wcy**	380	421	1.25
1mdy	337	485	0.06	**1wdy**	387	490	0.57

[a] I_R = Emission intensity of modified resin/Emission intensity of native resin **1m** or **1w**.
[b] In parentheses: the relative intensity of modified resins used to anchor **1mpy**.
[c] The maximum *wavelength of emission* was chosen at the midpoint of the parabola (vertex).

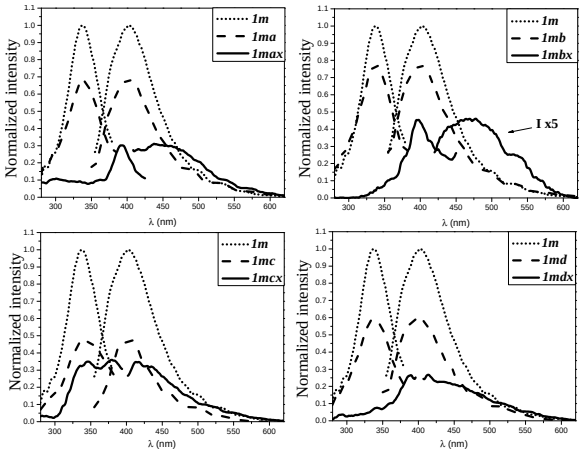

Fig. 1. Fluorescence spectra of Merrifield resin: native (**1m**), modified with diamine spacers [**1m(a-d)**] and functionalized with the ligand (**ttha1py**)$\mathbf{H_4}$ [**1m(a-d)x**]. The emission and excitation spectra of resin **1mbx** are shown amplified (Ix5).

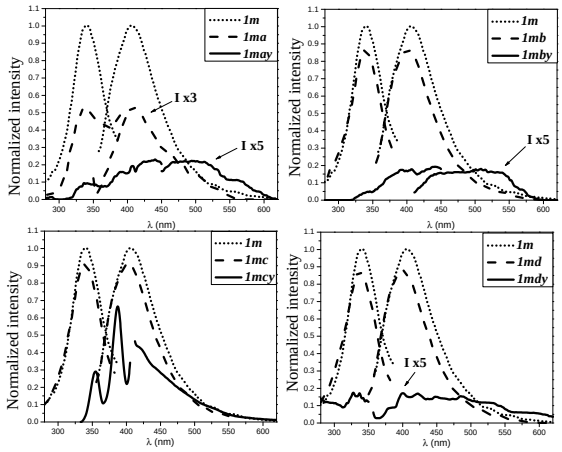

Fig. 2. Fluorescence spectra of Merrifield resin: native (**1m**), modified with diamine spacers [**1m(a-d)**] and functionalized with ligand (**ttha1mpy**)$\mathbf{H_4}$ [**1m(a-d)y**]. The emission and excitation spectra of resins **1ma** and [**1m(a,b,d)y**] are shown amplified (Ix3 and Ix5, respectively).

The schematic representation of the whole procedure is shown in Scheme 1. The infrared spectra of the final products showed two peaks that are characteristic of the stretching bands of the carbonyl group, the first peak located between 1646 and 1710 cm^{-1} and the second peak located between 1602 and 1680 cm^{-1}. The IR spectra also showed a wide peak corresponding to N−H amide between 3386 and 3446 cm^{-1} (Figures A5-A8).

These results indicated that the ligands **1py** and **1mpy** were successfully attached to the resins.

3.2 Fluorimetric characterization of materials

Merrifield and Wang resins functionalized with alkyl diamines **1**(**m**,**w**)(**a** – **d**) and the final products **1**(**m**,**w**)(**a** – **d**)(**x**,**y**) were transferred to a flow-through fluorescence microcell (8 μL) and spectra were obtained directly from the dry resins beads. The presence of alkyl diamines led to a decrease in the emission intensity of the native resins and small shifts in excitation and emission wavelengths (Figures 1-4 and Table 3).

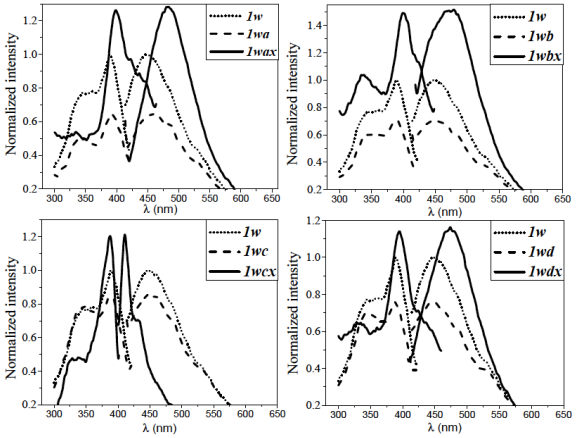

Fig. 3. Fluorescence spectra of Wang resin: native (**1w**), modified with diamine spacers [**1w(a-d)**] and functionalized with ligand (**ttha1py**)$\mathbf{H_4}$ [**1w(a-d)x**].

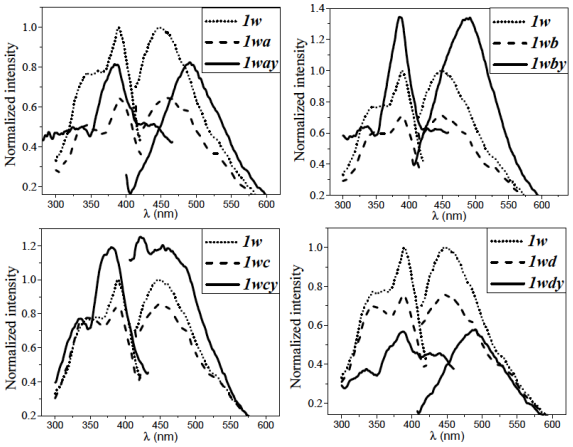

Fig. 4. Fluorescence spectra of Wang resin: native (**1w**), modified with diamine spacers [**1w(a-d)**] and functionalized with ligand (**ttha1mpy**)$\mathbf{H_4}$ [**1w(a-d)y**].

Incorporation of ligands **1py** or **1mpy** to alkyl diamine-modified Merrifield and Wang resins dramatically changes the fluorescence spectra of materials. The intensity, shape and maximum wavelenght of emission bands vary in each material (Figures 1-4 and Table 3). Except resin **1wcx**, whose spectrum is characteristic of monomeric pyrene, and resin **1mcy**, that showed only an emission tail extending from 425 nm approximately, the final products showed emission bands broad and shifted to red, with respect to those of the alkyl diamine derivatives, which resemble the emission spectra of **1py** or **1mpy** in solution (Pérez-González *et al*., 2011). The emission intensity of materials derived of Merrifield resin was significantly lower than that of native resin (Figures 1 and 2, and Table 3). In contrast, most of the materials derivated of Wang resin showed higher emission intensity than the native resin (Figures 3 and 4, and Table 3). A broad and well defined fluorescence band (λ_{max}= 479-491 nm) characteristic of pyrene excimer was observed in the spectra of most of the materials.

The most emissive resin was **1wbx** with I_R=1.51 (Table 3). The higher emission intensity of Wang derivatives, compare to that of the Merrifield materials, may be due to a higher percent of functionalization of the active sites with the fluorescent ligands. A lower cross-linked of the Wang resin respect to Merrifield resin and therefore a higher swelling in the solvent, allows a better diffusion of the ligands into the resin during the syntheses of the materials (Rana *et al*., 2001).

3.3 Sensing properties of materials toward Pb^{2+}, Cd^{2+} and Hg^{2+} ions

In order to evaluate the analytical potential of final products as sensing materials of Pb^{2+}, Cd^{2+} and Hg^{2+} ions, resins [**1**(**m**, **w**)(**a** – **d**)(**x**, **y**)] were put in contact during 48 h with aqueous solutions of the metals, at constant pH and temperature. The solids were separated by filtration, washed with water and dried under vacuum, and then packed into a flow-through fluorescence microcell to acquire the spectra. Figures 5 and 6 show the changes in fluorescence intensity of materials derived from Merrifield resin, after their interaction with Pb^{2+}, Cd^{2+} and Hg^{2+}. The spectra are shown in Appendix B, Figures B1 and B2. Most of derivatives have either moderate increases in intensity or quenching of fluorescence after metal coordination.

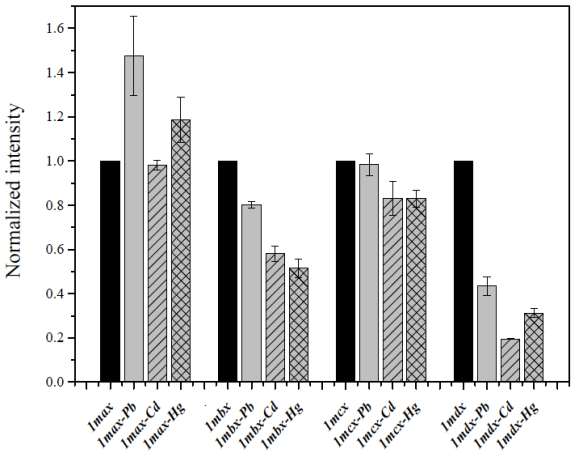

Fig. 5. Normalized fluorescence intensities of the materials [**1m(a-d)(x)**] before and after complexation to ions Pb^{2+}, Cd^{2+} and Hg^{2+}. The intensities were measured at wavelength of maximum of emission of the corresponding resin before contact with the metals in this experiment (λ_{em}= 470, 472, 410 y 473 nm for **1max**, **1mbx**, **1mcx** and **1mdx**, respectively). The intensities are presented as the mean ± standard deviation of three replicates.

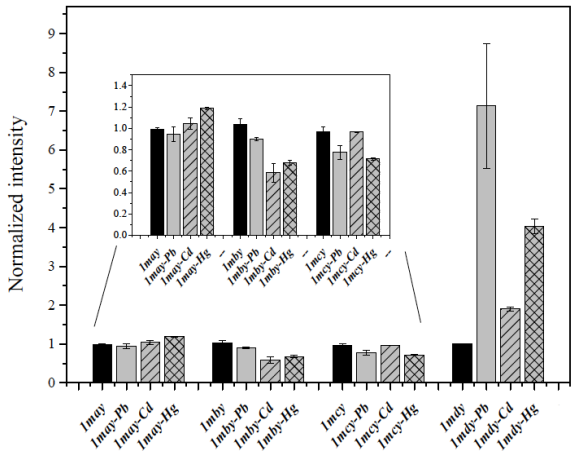

Fig. 6. Normalized fluorescence intensities of the materials [**1m(a-d)(y)**] before and after complexation to ions Pb^{2+}, Cd^{2+} and Hg^{2+}. The intensities were measured at wavelength of maximum of emission of the corresponding resin before contact with the metals in this experiment (λ_{em}= 466, 493, 418 y 489 nm for **1may**, **1mby**, **1mcy** and **1mdy**, respectively). The intensities are presented as the mean ± standard deviation of three replicates.

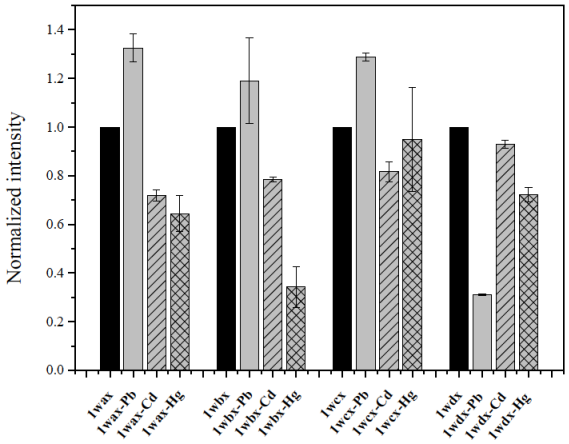

Fig. 7. Normalized fluorescence intensities of the materials [**1w(a-d)(x)**] before and after complexation to ions Pb^{2+}, Cd^{2+} and Hg^{2+}. The intensities were measured at wavelength of maximum of emission of the corresponding resin before contact with the metals (λ_{em}= 471, 460, 412 and 487 nm for **1wax**, **1wbx**, **1wcx** and **1wdx**, respectively). The intensities are presented as the mean ± standard deviation of three replicates.

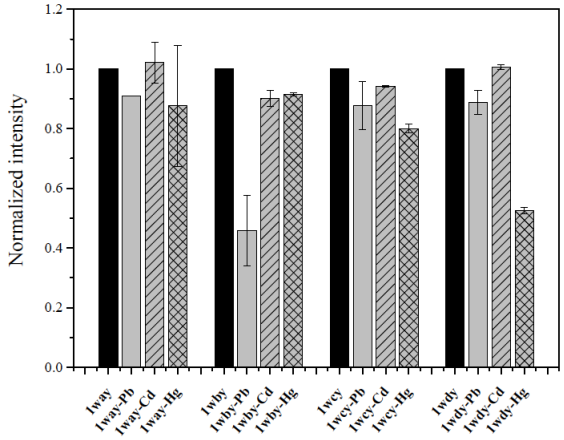

Fig. 8. Normalized fluorescence intensities of the materials [**1w(a-d)(y)**] before and after complexation to ions Pb^{2+}, Cd^{2+} and Hg^{2+}. The intensities were measured at wavelength of maximum of emission of the corresponding resin before contact with the metals (λ_{em}= 490 nm for **1way**, **1wby**, **1wdy**, and 455 nm for **1wcy**). The intensities are presented as the mean ± standard deviation of three replicates.

The exception is the resin **1mdy**, which showed a significant increase in fluorescence intensity due to the coordination of metals ions (Figure B2). The spectra of complexes **1mdy**-Pb and **1mdy**-Hg show intense peaks of monomeric pyrene between 350 and 450 nm,

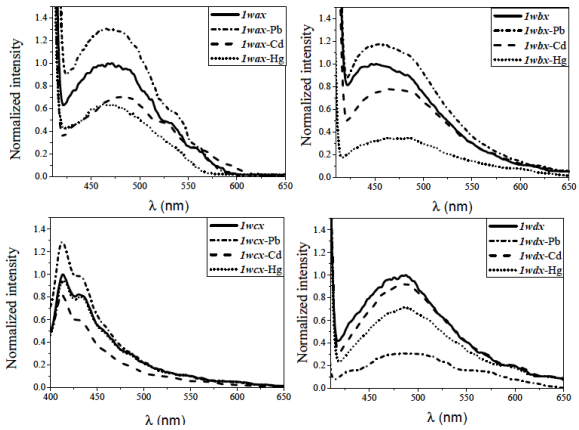

Fig. 9. Emission spectra of materials [**1w(a-d)x**] before and after coordination with the metal ions Pb^{2+}, Cd^{2+} and Hg^{2+} (λ_{exc}= 398, 399, 387 and 395 nm for **1wax**, **1wbx**, **1wcx** and **1wdx** respectively).

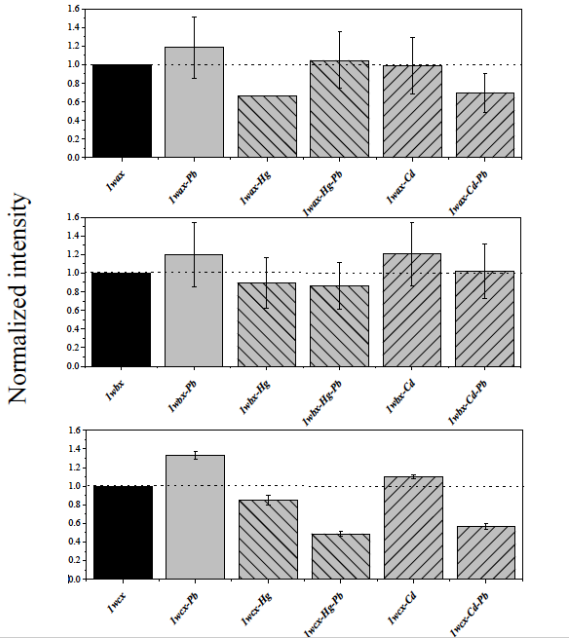

Fig. 10. Normalized fluorescence intensities of resins **1w(a-c)x** before and after treatment with ions Hg^{2+} and Cd^{2+} independently, and with both metals in the indicated order: Hg−Pb and Cd−Pb (for details see text). The emission intensities of resins treated with Pb^{2+} independently are shown for comparison purposes. The intensities were measured at wavelength of maximum of emission of the corresponding resin before contact with the metals (λ_{em}= 479, 503 and 409 nm for **1wax**, **1wbx** and **1wcx**, respectively). The intensities are presented as the mean ± standard deviation of two replicates.

Table 4. Relative intensities of fluorescence (I/I_0) of materials [**1(m,w)(a-d)(x,y)**] upon complexation to ions Pb^{2+}, Cd^{2+} y Hg^{2+} .[a,b]

Material	Metal ion			Material	Metal ion		
	Pb^{2+}	Cd^{2+}	Hg^{2+}		Pb^{2+}	Cd^{2+}	Hg^{2+}
1max	1.4	0.98	1.25	**1wax**	1.32	0.71	0.64
1mbx	0.8	0.61	0.55	**1wbx**	1.19	0.78	0.34
1mcx	0.94	0.82	0.8	**1wcx**	1.28	0.81	0.94
1mdx	0.41	0.19	0.31	**1wdx**	0.31	0.92	0.72
1may	0.94	1.04	1.18	**1way**	0.9	1.02	0.87
1mby	0.89	0.58	0.67	**1wby**	0.45	0.9	0.91
1mcy	0.77	0.96	0.71	**1wcy**	0.87	0.94	0.79
1mdy	7.13	1.9	4.02	**1wdy**	0.88	1	0.52

[a] I_0 and I stand for intensities before and after metal coordination.
[b] The intensities were measured at wavelength of maximum of emission of the corresponding resin before contact with the metals (see details in Figures 5-8).

and the broad band characteristic of pyrene excimers at 480 nm.

The ratios I/I_0 at 480 nm (where I_0 and I stand for intensities before and after metal coordination) reach the values 7.13 and 4.02 for Pb^{2+} and Hg^{2+}, respectively.

In the case of **1mdy**-Cd, the spectrum shows predominantly excimer emission, with a value of I/I_0 =1.90 at 480 nm (see Table 4 and Figure B2). Figures 7 and 8 show the changes in fluorescence intensity of materials derived from Wang resin, after their interaction with Pb^{2+}, Cd^{2+} and Hg^{2+}. Resins **1w(a – c)x** are distinguishing by show an increase in emission intensity by coordination to Pb^{2+} and a quenching of fluorescence by effect of Cd^{2+} and Hg^{2+} (the spectra are shown in Figure 9). This selectivity to Pb^{2+} is not shown by the rest of the materials, whose fluorescence intensity decreases by effect of coordination to the three metal ions (see Table 4 and Figure B3). To investigate the possible interference of Cd^{2+} and Hg^{2+} in the fluorescence enhancement induced by Pb^{2+} in the resins **1w(a – c)x**, we carried out a competition study with binary mixtures in independent assays. The resins were first put in contact with the competitor metal ion (Cd^{2+} or Hg^{2+}) and subsequently treated with Pb^{2+}. In addition, each material was treated independently with Pb^{2+} to be used it as reference. The results are shown in Figure 10. Resin **1wax** is the only one that maintains the increase in fluorescence intensity by coordination to Pb^{2+}, in presence of the competitor metal, specifically Hg^{2+}. The shape and position of the emission band of **1wax**, which is characteristic of pyrene excimers, remains unchanged during the test, and only variations in fluorescence intensity were observed (Figure 11).

The above results prompted us to test the selectivity of the resin **1wax** to Pb^{2+} in presence of the two competitor metals, Cd^{2+} and Hg^{2+}. The material was first put in contact with the competing metals sequentially (first with Hg^{2+} and then with Cd^{2+}) and finally treated with Pb^{2+}. The sequence in the treatment with the metal cations was the following: Hg, Hg−Cd and Hg−Cd−Pb. In addition, resin **1wax** was treated independently with Pb^{2+} to be used it as reference.

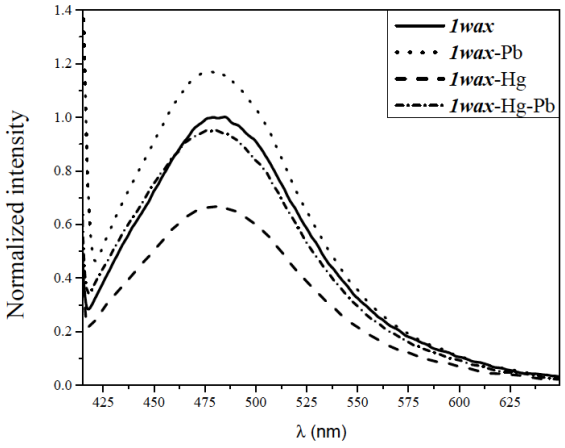

Fig. 11. Emission spectra (λ_{exc}= 398 nm) of resin **1wax** before and after treatment with Hg^{2+} and Hg^{2+}−Pb^{2+} (for details see text). The spectrum of material treated with Pb^{2+} independently is shown for comparison purposes.

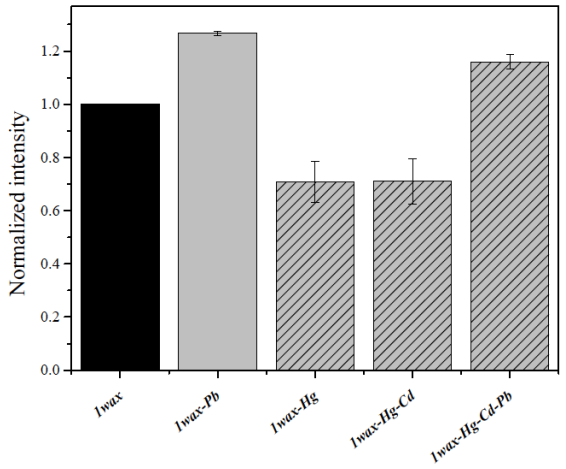

Fig. 12. Normalized fluorescence intensities at 479 nm (λ_{exc}= 398 nm) of resin **1wax** before and after treatment with Hg^{2+}, Cd^{2+} and Pb^{2+} in the order indicated: Hg, Hg−Cd and Hg−Cd−Pb (for details see text). The emission intensity of resin treated with Pb^{2+} independently is shown for comparison purposes.

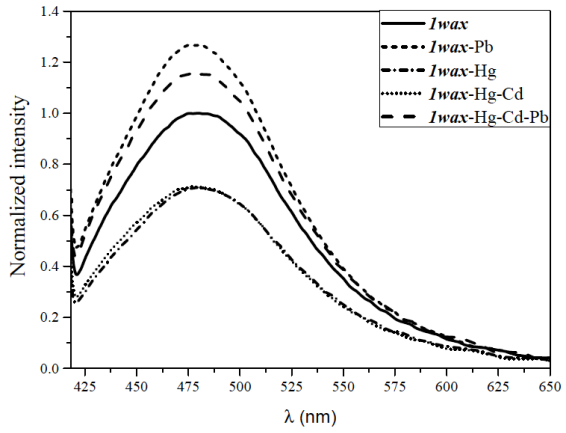

Fig. 13. Emission spectra (λ_{exc}= 398 nm) of resin **1wax** before and after treatment with Hg^{2+}, Hg^{2+}−Cd^{2+} and Hg^{2+}−Cd^{2+}−Pb^{2+} (for details see text). The spectrum of material treated with Pb^{2+} independently is shown for comparison purposes.

As shown in Figure 12, the resin **1wax** maintains the increase in fluorescence intensity by contact with Pb^{2+}, even after being treated with the Hg^{2+} and Cd^{2+} ions, which cause a quenching of the fluorescence of the material. The intensities are presented as the mean ± standard deviation of two replicates. As in the previous test, the pyrene excimer band of **1wax** remains unchanged during the different stages of the assay, and only variations in fluorescence intensity were observed (Figure 13).

These results indicate the potential for application of the resin **1wax** as a selective fluorescent sensor for Pb^{2+} in contaminated water. The increase in emission intensity at 480 nm can be easily measured and used to detect the presence of the highly toxic ion Pb^{2+}, even in presence of the other contaminants. To establish the sensitivity of the resin **1wax** to Pb^{2+}, the detection limit (*DL*) was determined accordingly to methodology describe in the literature (Lohani *et al*., 2012; Thirupathi and Lee, 2013; Yang *et al*., 2011). The *DL* was calculated as 29.6 μM with the following equation:

$$DL = 3\sigma/m \quad (1)$$

where σ is the standard deviation of blank measurements (n=10, σ = 0.8098) and m is the slope of the plot of intensity versus Pb^{2+} concentration (see Experimental and Figure C1 in Appendix C). This result indicates that the resin can be used to detect low levels of Pb^{2+} in aqueous solutions.

3.4 *Sorption properties of* **1wax** *toward* Pb^{2+} *ion*

Once stablished the properties of resin **1wax** as a fluorescent sensor of Pb^{2+}, it was determined its capacity to remove this highly toxic metal ion from aqueous media. This due to the interest that currently exist in developing efficient methods for the capture of metal pollutants from effluents that are discharged into bodies of water such as lakes, rivers and the sea (Badillo-Camacho *et al*., 2016; Orozco *et al*., 2011). The lead removal capacity of the resin **1wax** was determined as percentage of sorption (% Sorption) using the column technique, accordingly to methodology describe in Experimental. The value obtained was 80.3%, which indicates a high capacity of the resin to remove that metal from contaminated aqueous solutions. Moreover, the stability and regeneration capacity of **1wax** remain almost unaltered after 10 cycles sorption-desorption (Figure C2).

Conclusions

In conclusion, we prepared a combinatorial library of 16 fluorescent materials by covalent anchoring of 1-pyrene and 1-methylpyrene bichromophores to Merrifield and Wang resins functionalized with alkyl diamine spacers of different length. The fluorescence

and the sensing properties in water of these materials toward the toxic metal ions Pb^{2+}, Cd^{2+} and Hg^{2+} were studied. It was found that the Wang resin modified with ethane-1,2-diamine as spacer and functionalized with (**ttha1py**)$\mathbf{H_4}$, **1wax**, senses selectively Pb^{2+} with an enhancement of fluorescence intensity. The resin maintains the fluorescent response toward Pb^{2+}, even in presence of Hg^{2+} and Cd^{2+}. The detection limit and the percentage of sorption toward Pb^{2+} of **1wax** were determined as 29.6 μM and 80.3%, respectively. The resin shows a high stability and regeneration capacity. These results indicate the potential for application of the resin **1wax** as a selective fluorescent sensor for Pb^{2+} and as an effective material for the separation of traces of metal ions in contaminated water.

Acknowledgements

This work was supported in part by the Consejo Nacional de Ciencia y Tecnología de México (CONACYT, Project No. 79272 and RTQS 294810). The authors thank Dr. Mario Enrique Alvarez Ramos and Dr. Roberto Carrillo Torres by the access to the Raman microscope. J.E. Ávila-Manzanares thanks CONACYT for graduate scholarship.

Abbreviations

C_i	initial concentration of Pb^{2+} in the standard solution
C_f	final concentration after the sorption
I_R	emission intensity of modified resin/emission intensity of native resin **1m** or **1w**
I_0	intensities before metal coordination
I	intensities after metal coordination
DL	detection limit
σ	standard deviation of blank measurements
m	slope of the plot

References

Aguilar-Martínez, M., J. Vargas-Durazo, K. L. Ochoa-Lara, H. Santacruz-Ortega, and J. C. Gálvez-Ruiz. (2013). Merrifield and wang resins functionalized with bidentate amines: Useful materials to support reducing complexes and as alkali metal sensors. *Zeitschrift für Anorganische und Allgemeine Chemie 639*, 1166-1172.

Akhila Maheswari, M., and M. S. Subramanian. (2003). Selective extraction of U(VI) and Th(IV) from high saline matrices using AXAD-16-BHBPD as chelating polymeric matrix. *Analytical Letters 36*, 2875-2892.

Avila M., J. E. (2012). *Estudios de coordinación metálica de dos nuevos quimiosensores fluorescentes derivados del ttha, funcionalizados con grupos pireno*. Universidad de Sonora.

Badillo-Camacho, J., J. O. Murillo-Delgado, I. D. Barcelo-Quintal, P. F. Zarate del Valle, E. Orozco-Guareño, U. J. López-Chuken, and S. Gomez-Salazar. (2016). Heavy metals speciation in sediments of a Mexican tropical lake. *Revista Mexicana de Ingeniería Química 15*, 565-573.

Brown, G. J., A. P. de Silva, M. R. James, B. O. F. McKinney, D. A. Pears, and S. M. Weir. (2008). Solid-bound, proton-driven, fluorescent “off-on-off" switches based on PET (photoinduced electron transfer). *Tetrahedron 64*, 8301-8306.

Castillo, M., and I. A. Rivero. (2004). Combinatorial synthesis of fluorescent trialkylphosphine sulfides as sensor materials for metal ions of environmental concern. *Arkivoc 2003*, 193-202.

Chen, K.-H., C.-Y. Lu, H.-J. Cheng, S.-J. Chen, C.-H. Hu, and A.-T. Wu. (2010). A pyrenyl-appended triazole-based ribose as a fluorescent sensor for Hg^{2+} ion. *Carbohydrate Research 345*, 2557-2561.

Gaggini, F., A. Porcheddu, G. Reginato, M. Rodriquez, and M. Taddei. (2004). Colorimetric tools for solid-phase organic synthesis. *Journal of Combinatorial Chemistry 6*, 805-810.

Hou, C., Y. Xiong, N. Fu, C. C. Jacquot, T. C. Squier, and H. Cao. (2011). Turn-on ratiometric fluorescent sensor for Pb^{2+} detection. *Tetrahedron Letters 52*, 2692-2696.

Hung, H.-C., C.-W. Cheng, I. T. Ho, and W.-S. Chung. (2009). Dual-mode recognition of transition metal ions by bis-triazoles chained pyrenes. *Tetrahedron Letters 50*, 302-305.

Joshi, B. P., W.-M. Cho, J. Kim, J. Yoon, and K.-H. Lee, (2007). Design, synthesis, and evaluation of peptidyl fluorescent probe for Zn2+ in

aqueous solution. *Bioorganic & Medicinal Chemistry Letters 17*, 6425-6429.

Joshi, B. P., J.-Y. Park, and K.-H. Lee, (2014). Recyclable sensitive fluorimetric detection of specific metal ions using a functionalized PEG-PS resin with a fluorescent peptide sensor: Sensors and Actuators B. *Chemical 191*, 122-129.

Kara, D., (2005). Separation and removal of mercury(II) from water samples using (acetylacetone)-2-thiol-phenyleneimine immobilized on anion-exchange resin prior to determination by cold vapor inductively coupled plasma atomic emission spectroscopy. *Analytical Letters 38*, 2217-2230.

Larkin, P., (2011). *Infrared and Raman Spectroscopy; Principles and Spectral Interpretation*. Elsevier Science.

Lodeiro, C., J. C. Lima, A. J. Parola, J. S. Seixas de Melo, J. L. Capelo, B. Covelo, A. Tamayo, and B. Pedras, (2006). Intramolecular excimer formation and sensing behavior of new fluorimetric probes and their interactions with metal cations and barbituric acids: Sensors and Actuators B. *Chemical 115*, 276-286.

Lohani, C. R., L. N. Neupane, J.-m. Kim, and K.-H. Lee, (2012). Selectively and sensitively monitoring Hg^{2+} in aqueous buffer solutions with fluorescent sensors based on unnatural amino acids. Sensors and Actuators B. *Chemical 161*, 1088-1096.

Machi, L., I. C. Muñoz, R. Pérez-González, M. Sánchez, and M. Inoue, (2009). Pyrene bichromophores composed of polyaminopolycarboxylate interlink: pH response of excimer emission. *Supramolecular Chemistry 21*, 665-673.

Manandhar, E., and K. J. Wallace, (2012), Host-guest chemistry of pyrene-based molecular receptors. *Inorganica Chimica Acta 381*, 15-43.

Narin, I., M. Soylak, K. Kayakirilmaz, L. Elci, and M. Dogan, (2003), Preparation of a chelating resin by immobilizing 1-(2-Pyridylazo) 2-Naphtol on amberlite XAD-16 and its application of solid phase extraction of Ni(II), Cd(II), Co(II), Cu(II), Pb(II), and Cr(III) in natural water samples. *Analytical Letters 36*, 641-658.

Nath, S., and U. Maitra, (2006). A simple and general strategy for the design of fluorescent cation sensor beads. *Organic Letters 8*, 3239-3242.

Orozco, E., S. L. Hernández, S. Gomez-Salazar, E. Mendizabal, and I. Katime, (2011). Study of acrylic terpolymeric hydrogels swelling in water and aqueous solutions containing lead(II) Ions. *Revista Mexicana de Ingeniería Química 10*, 465-470.

Prabhakaran, D., and M. S. Subramanian, (2003). Chemically modified chloromethylated resin as an effective metal chelator in the extraction of U(VI) and Th(IV). *Analytical Letters 36*, 2277-2289.

Pérez-González, R., L. Machi, M. Inoue, M. Sánchez, and F. Medrano, (2011). Fluorescence and conformation in water-soluble bis(pyrenyl amide) receptors derived from polyaminopolycarboxylic acids. *Journal of Photochemistry and Photobiology A: Chemistry 219*, 90-100.

Rana, S., P. White, and M. Bradley, (2001). Influence of resin cross-linking on solid-phase chemistry. *Journal of Combinatorial Chemistry 3*, 9-15.

Rivero, I. A., T. Gonzalez, G. Pina-Luis, and M. E. Diaz-Garcia, (2004). Library preparation of derivatives of 1,4,10,13-tetraoxa-7,16-diaza-cyclooctadecane and their fluorescence behavior for signaling purposes. *Journal of Combinatorial Chemistry 7*, 46-53.

Santacruz Ortega, H., G. Pina-Luis, S. Karime López, and I. A. Rivero, (2009). Preparation of a library of EDTA amide x-aminenaphthalene-y-sulfonic acid derivatives on solid phase and their fluorescence behavior toward transition metals. *Journal of Combinatorial Chemistry 11*, 1030-1037.

Thirupathi, P., and K.-H. Lee, (2013). A ratiometric fluorescent detection of Zn(II) in aqueous solutions using pyrene-appended histidine. *Bioorganic & Medicinal Chemistry Letters 23*, 6811-6815.

Xie, J., X. Liao, F.-Z. Qing, P. Luo, Z.-F. Zhang, J. Huang, and L.-S. Qing, (2014). A novel rhein-functionalized resin with application for the preconcentration of anthraquinones. *Analytical Letters 47*, 2332-2340.

Yan, B., H.-U. Gremlich, S. Moss, G. M. Coppola, Q. Sun, and L. Liu, (1998). A comparison of various FTIR and FT Raman methods: Applications in the reaction optimization stage of combinatorial chemistry. *Journal of Combinatorial Chemistry 1*, 46-54.

Yang, M.-H., P. Thirupathi, and K.-H. Lee, (2011). Selective and sensitive ratiometric detection of Hg(II) ions using a simple amino acid based sensor. *Organic Letters 13*, 5028-5031.

Zhou, Y., C.-Y. Zhu, X.-S. Gao, X.-Y. You, and C. Yao, (2010). Hg^{2+}-selective ratiometric and "Off-On" chemosensor based on the azadiene-pyrene derivative. *Organic Letters 12*, 2566-2569.

Appendix A

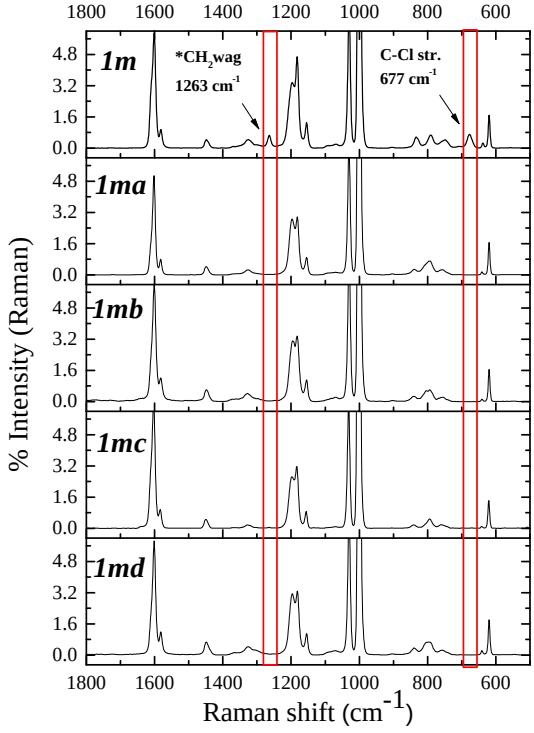

Fig. A1. Raman spectra of native Merrifield resin **1m** and modified with diamine spacers **1m(a-d)**. *The CH_2 wag band corresponds to CH_2−Cl group in Merrifield resin. The signals were normalized to the strongest signal, which was defined as 100%.

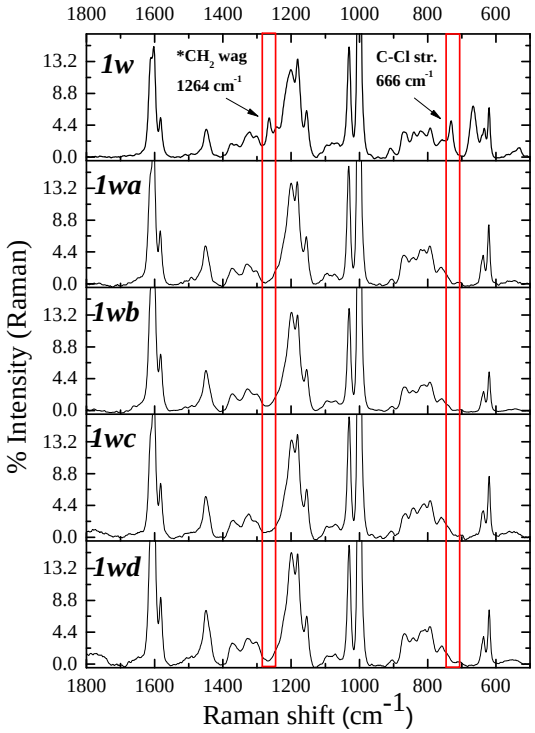

Fig. A2. Raman spectra of native Wang resin **1w** and modified with diamine spacers **1w(a-d)**. *The CH_2 wag band corresponds to CH_2−Cl group in Wang resin. The signals were normalized to the strongest signal, which was defined as 100%.

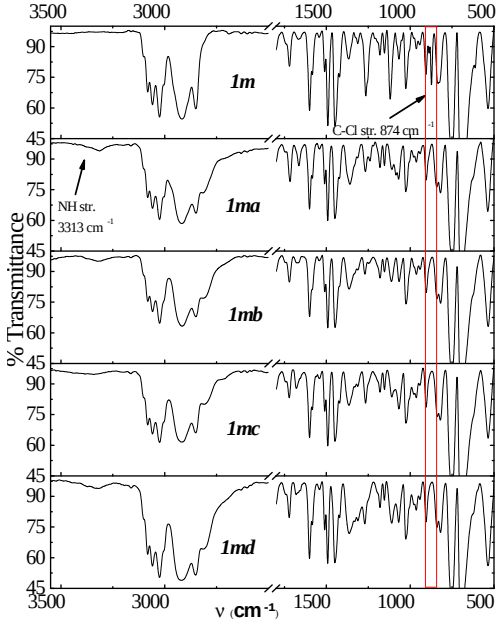

Fig. A3. Infrared spectra of native Merrifield resin **1m** and modified with diamine spacers **1m(a-d)**.

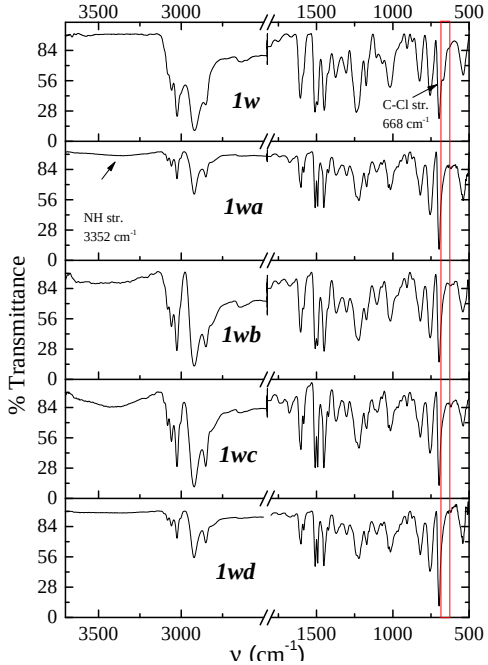

Fig. A4. Infrared spectra of native Wang resin **1w** and modified with diamine spacers **1w(a-d)**.

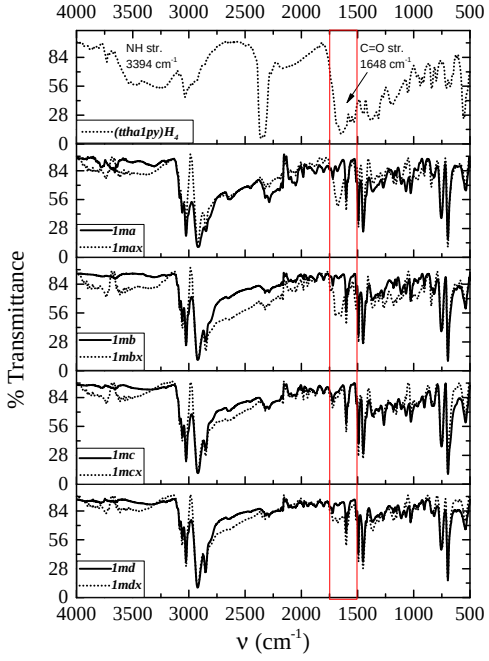

Fig. A5. IR spectra of Merrifield resins modified with diamine spacers [**1m(a-d)**] and of the final products [**1m(a-d)x**]. The IR spectra of the ligand (**ttha1py**)**H$_4$** is shown at top for comparison.

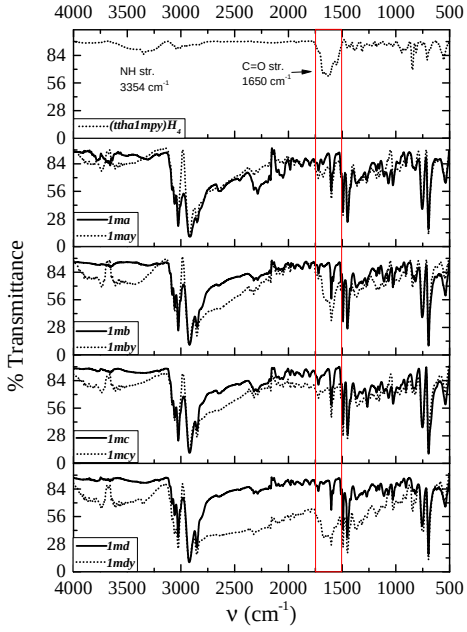

Fig. A6. IR spectra of Merrifield resins modified with diamine spacers [**1m(a-d)**] and of the final products [**1m(a-d)y**]. The IR spectra of the ligand (**ttha1py**)**H$_4$** is shown at top for comparison.

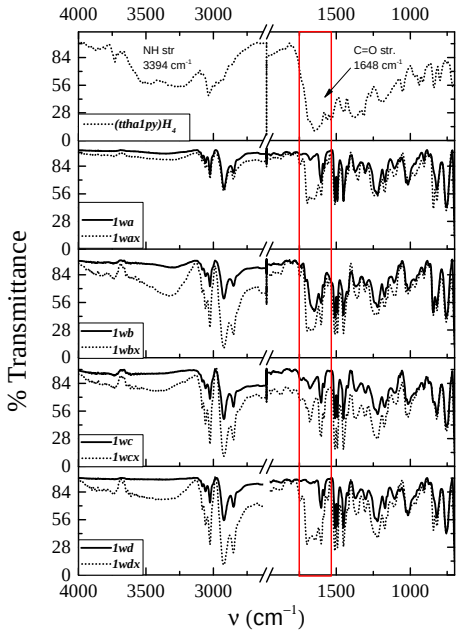

Fig. A7. IR spectra of Wang resins modified with diamine spacers [**1w(a-d)**] and of the final products [**1w(a-d)x**]. The IR spectra of the ligand (**ttha1py**)**H$_4$** is shown at top for comparison.

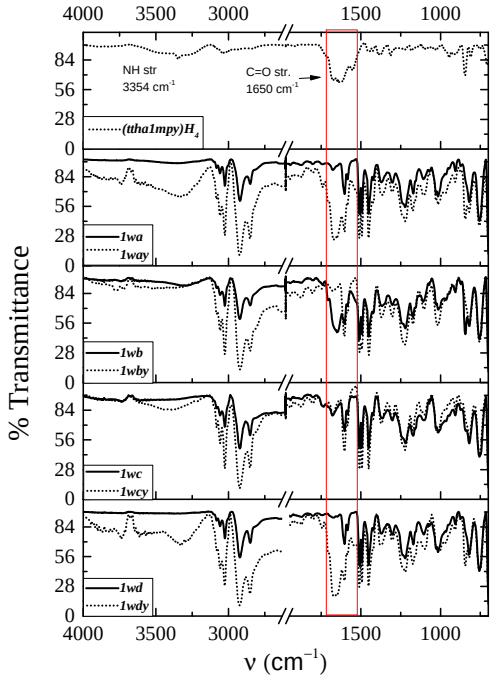

Fig. A8. IR spectra of Wang resins modified with diamine spacers [**1w(a-d)**] and of the final products [**1w(a-d)y**]. The IR spectra of the ligand (**ttha1py**)**H$_4$** is shown at top for comparison.

Appendix B

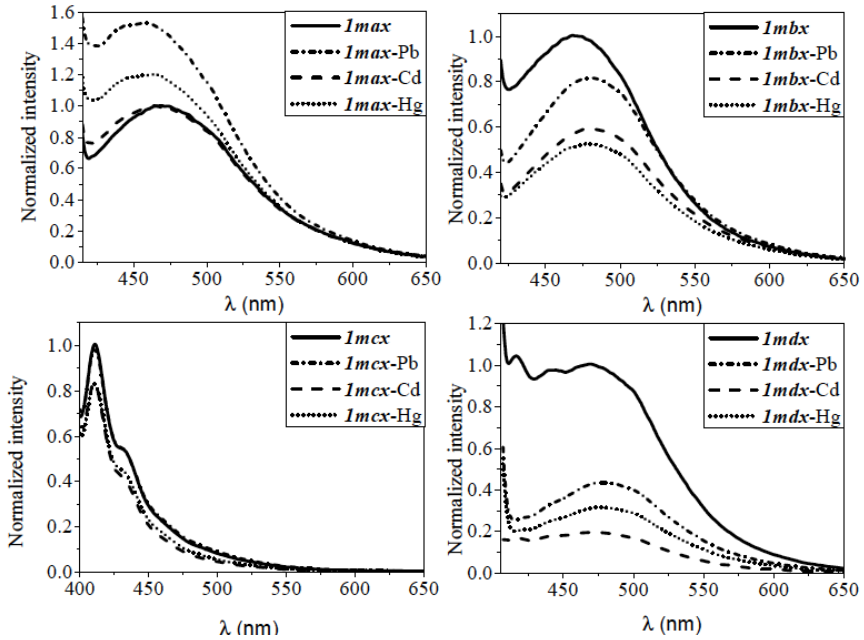

Fig. B1. Emission spectra of materials [**1m(a-d)x**] before and after coordination with the metal ions Pb^{2+}, Cd^{2+} and Hg^{2+} (λ_{exc} = 393, 397, 383 and 389 nm for **1max**, **1mbx**, **1mcx** and **1mdx**, respectively).

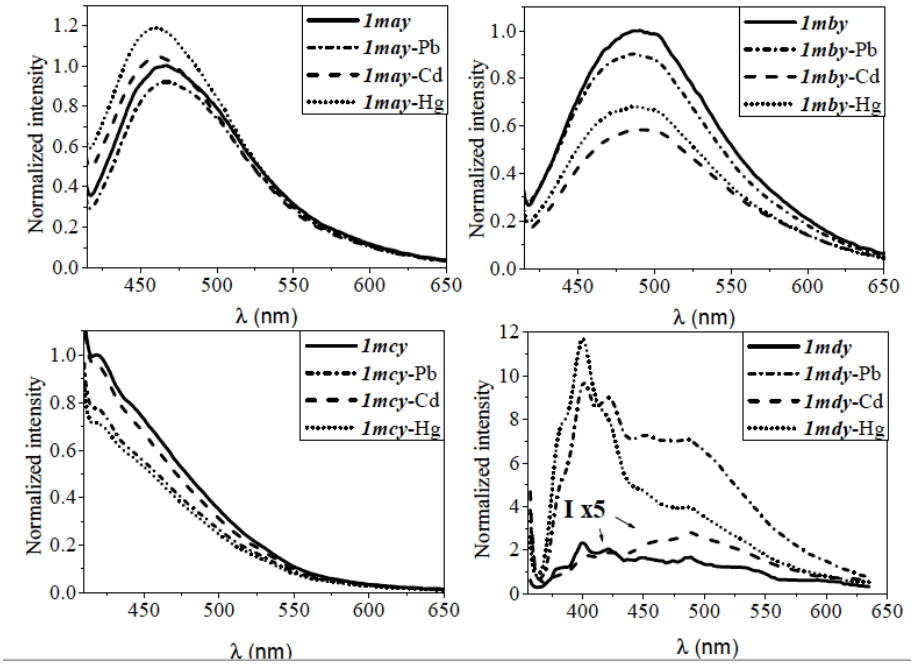

Fig. B2. Emission spectra of materials [**1m(a-d)y**] before and after coordination with the metal ions Pb^{2+}, Cd^{2+} and Hg^{2+} (λ_{exc}= 391 nm for **1may** and **1mby**, 387 nm for **1mcy** and 337 nm for **1mdy**). The emission spectra of resins **1mdy** and **1mdy**-Cd are shown amplified (Ix5).

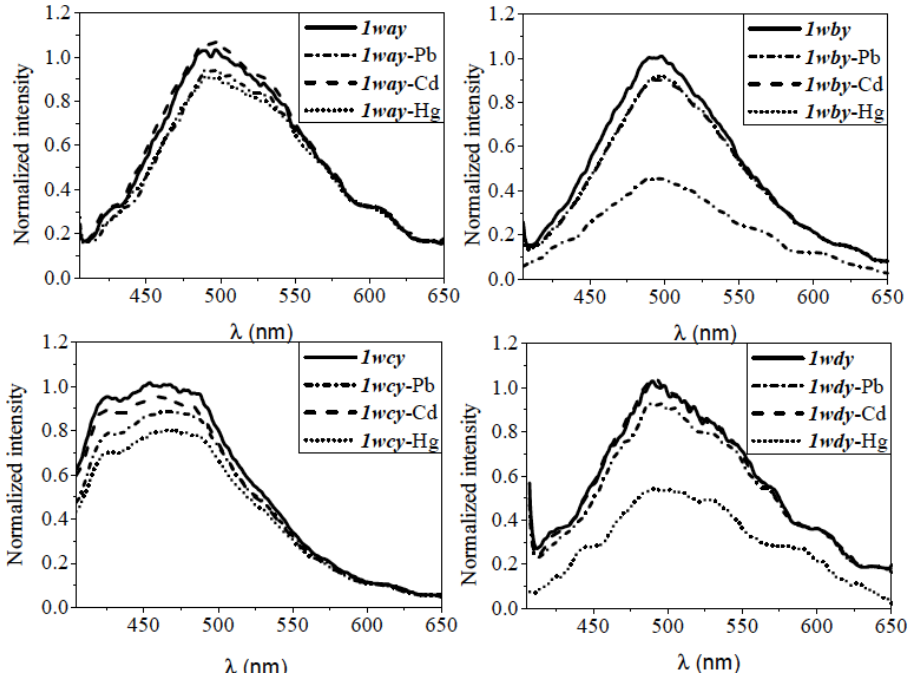

Fig. B3. Emission spectra of materials [**1w(a-d)y**] before and after coordination with the metal ions Pb^{2+}, Cd^{2+} and Hg^{2+} (λ_{exc}= 383, 385, 380 and 387 nm for **1way**, **1wby**, **1wcy** and **1wdy**, respectively).

Appendix C

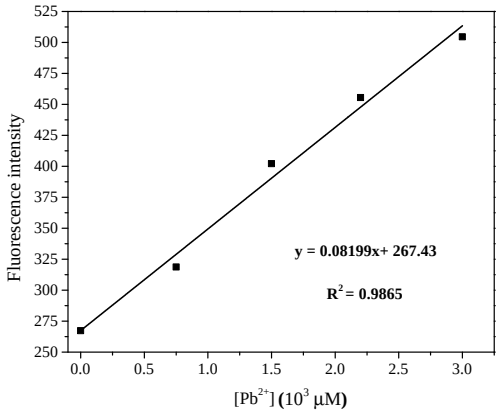

Fig. C1. Fluorescence intensity of **1wax** at λ_{em}= 471 nm as a function of concentration of Pb^{2+} (0-3000 μM) at pH 5 (MOPS). The solid lines show the linear regression of data.

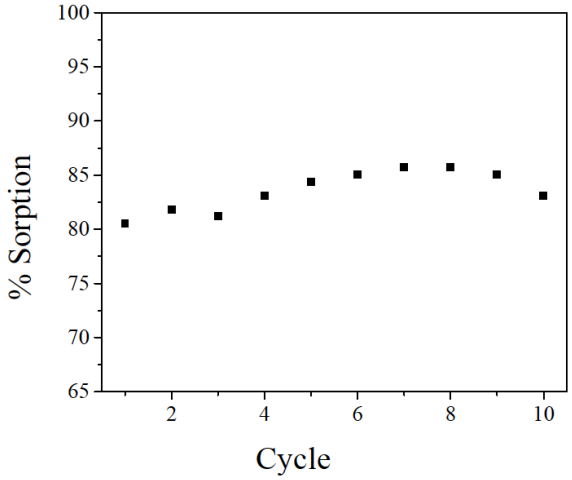

Fig. C2. Profile of reusability based on the percentage of sorption of **1wax** toward Pb^{2+} ion.